This article has been accepted for publication in a future issue of this journal, but has not been fully edited. Content may change prior to final publication. Citation information: DOI 10.1109/TWC.2018.2865313, IEEE Transactions on Wireless Communications

Wireless Power Transfer with Hybrid Beamforming: How Many RF Chains Do We Need?

Lu Yang, *Member, IEEE,* Yong Zeng, *Member, IEEE,* and Rui Zhang, *Fellow, IEEE*

***Abstract*—Wireless power transfer (WPT) via dedicated radio frequency (RF) transmission is an appealing technology to provide cost-effective energy supply to low-power devices in the future era of Internet of Things (IoT). To achieve efficient power delivery over moderate distance, WPT usually relies on highly directional power transmission from the energy transmitter (ET) to the energy receiver (ER). To this end, the ET needs to be equipped with a large number of antennas and employ adaptive energy beamforming to flexibly control the energy focusing directions to the ER based on the multipath channels between them. However, this renders the conventional fully digital beamforming with one dedicated RF chain for each transmit antenna too costly, in terms of both hardware implementation and energy consumption. To overcome this issue, we study in this paper a new WPT system based on the hybrid analog/digital beamforming technique, where the number of RF chains is in general significantly less than that of transmit antennas. We first show that for a general point-to-point multiple-input multiple-output (MIMO) WPT system over frequency-selective channels, hybrid beamforming is able to achieve the optimal performance as the fully digital beamforming, as long as the number of RF chains at the ET is no less than twice the number of sub-bands used or twice the number of channel paths. Furthermore, for the special cases of line-of-sight (LoS) channel or multiple-input single-output (MISO) WPT, the required number of RF chains can be further reduced to equal the number of channel paths only. Finally, for the scenarios when the given number of RF chains is insufficient to achieve the fully digital beamforming performance, we propose efficient algorithms for the hybrid beamforming design to maximize its efficiency. Numerical results are provided to validate our analytical results and demonstrate the effectiveness of the proposed hybrid beamforming design.**

***Index Terms*—Wireless power transfer, hybrid beamforming, MIMO, frequency-selective channel, limited RF chains.**

I. Introduction

Far-field wireless power transfer (WPT) based on radio frequency (RF) signal transmission is a promising technology to provide convenient and cost-effective energy supply to numerous low-power wireless devices in future Internet-of-Things (IoT), such as radio-frequency identification (RFID) tags, sensors, low-power electronics, etc [1], [2]. Compared to the counterpart near-field WPT technologies based on inductive coupling [3], [4] or magnetic resonant coupling [5], far-field WPT offers many advantages, such as significantly enhanced transmission range, substantially reduced transmitter/receiver size, more flexibility in transmitter/receiver deployment, capability of providing concurrent power delivery to multiple devices, and applicability even in non-line-of-sight (NLoS) environment. Therefore, it is anticipated that RF-based WPT will play an important role in future IoT systems.

However, WPT systems are also faced with many new challenges, which, if not tackled successfully, could roadblock their wide applications in practice. In particular, one critical challenge lies in how to enhance the end-to-end power transfer efficiency from the energy transmitter (ET) to the energy receiver (ER), which is fundamentally limited by the low received RF power at the ER due to the severe signal attenuation over distance. To this end, WPT systems usually rely on highly directional transmission at the ET, by essentially pinpointing the transmitted RF power towards the designated ER. This was historically achieved by using bulky transmit antennas, such as parabolic dish antenna with 26 meters in diameter for the JPL Goldstone demonstration [6]. For such systems, the antenna orientation needs to be mechanically adjusted to focus the signal towards the ER and a clear line-of-sight (LoS) link between the ET and ER is required. On the other hand, to achieve more flexible directional power transmission in the more challenging non-LoS (NLoS) environment, WPT systems using electronically steerable antenna arrays have been studied recently [7]–[18]. In this case, the ET is equipped with multiple or even a massive number of antenna elements, and the amplitude and phase of the energy signals transmitted by different antennas are adaptively designed based on the multi-path channels to achieve constructive signal superposition at one or more intended ERs, a technique known as *energy beamforming* [7]. With optimal energy beamforming, the received RF power at the ER in principle increases proportionally with the number of transmit antennas. Besides energy beamforming, another promising technique for WPT systems with a large available bandwidth over multi-path channels is to exploit the frequency-diversity gain [19]–[22], e.g., by transmitting more power over the sub-bands with higher channel gains.

Existing works on multi-antenna WPT systems are mostly based on the fully digital beamforming architecture, where each transmit antenna is connected with one dedicated RF chain so that both the amplitude and phase of the transmitted

Manuscript received December 18 2017, revised March 28 2018 and June 13 2018, accepted August 07 2018. This work was supported by the National University of Singapore under Research Grant R-263-000-B62-112. The associate editor coordinating the review of this paper and approving it for publication was M. Cenk Gursoy. (*Corresponding author: Yong Zeng*.)

L. Yang is with the School of Electrical Engineering and Telecommunications, The University of New South Wales, Australia (e-mail: lu.yang@unsw.edu.au).

Y. Zeng was with the Department of Electrical and Computer Engineering, National University of Singapore, Singapore 117583, and now with the School of Electrical and Information Engineering, The University of Sydney, NSW, Australia, 2006 (Email: yong.zeng@sydney.edu.au).

R. Zhang is with the Department of Electrical and Computer Engineering, National University of Singapore, Singapore 117583 (e-mail: elezhang@nus.edu.sg).

This article has been accepted for publication in a future issue of this journal, but has not been fully edited. Content may change prior to final publication. Citation information: DOI 10.1109/TWC.2018.2865313, IEEE Transactions on Wireless Communications

signal at each antenna can be flexibly adjusted in baseband. However, as the number of antennas at the ET increases, the conventional fully digital beamforming based WPT system becomes too costly in terms of both hardware implementation and energy consumption due to the large number of required RF chains. Note that there are also similar issues for the emerging massive MIMO wireless communication systems with very large number of transmit antennas, especially at millimeter wave (mmWave) frequencies with large signal bandwidth [23]–[28]. One appealing approach to reduce the RF chain cost in large-array communication systems is to adopt the hybrid analog/digital beamforming architecture [29], [30], where a limited number of RF chains are connected with the large antenna arrays via power splitters and a network of analog phase shifters. Such an architecture combines the digital processing in baseband and analog beamforming in RF band to achieve cost reduction. Compared with the conventional fully digital beamforming, the design of hybrid beamforming needs to take into account two new practical considerations. The first one is the constant-modulus constraint on the transmit signal from each element of the analog beamformers. The second one is the frequency-flat analog beamforming over the parallel frequency sub-bands, i.e., unlike digital beamforming where independent beamforming coefficients can be used for different sub-bands, the analog beamforming coefficients need to be identical across all sub-bands since they are implemented in the RF domain. Hybrid analog/digital beamforming has been extensively studied for wireless communication systems over both narrow-band [31], [32] and orthogonal frequency-division multiplexing (OFDM) based wide-band channels [35], [36]. Recently, hybrid beamforming has also been studied for simultaneous wireless information and power transfer (SWIPT) systems [37], [38]. In particular, the work in [37] investigated the joint design of hybrid beamforming and power splitting ratio for a multi-user SWIPT system, so as to minimize the transmit power while satisfying both the signal-to-interference-plus-noise ratio (SINR) and harvested power constraints. The work in [38] considered the SWIPT scenario with one information receiver and multiple energy receivers, where it is shown that the optimal beamformer consists of only information beamformer. To the authors' best knowledge, the application of hybrid beamforming for cost-effective WPT systems has not been investigated yet in the literature.

In this paper, we study a point-to-point multiple-input multiple-output (MIMO) WPT system over the general frequency-selective channels with hybrid analog/digital beamforming at the ET, as shown in Fig. 1. Note that due to the fundamentally different design objectives for wireless communication and WPT systems (rate versus power maximization), the existing results for hybrid beamforming in wireless communication systems cannot be directly applied for WPT systems. For instance, it has been shown in [29] and [32] that for narrow-band wireless communication systems, hybrid beamforming is able to achieve the same optimal performance as the fully digital beamforming, provided that the number of RF chains is twice as that of the transmitted data streams. However, it is not immediately clear whether a similar result exists for WPT systems, especially for multi-band WPT that exploits frequency diversity gains. This thus motivates the current work. The main contributions of this paper are summarized as follows.

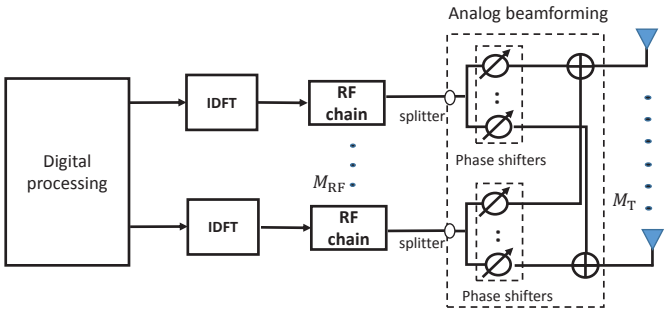

Fig. 1: Schematics of MIMO WPT over multi-band channels with hybrid beamforming.

First, we present the hybrid analog/digital beamforming architecture for WPT systems over the general MIMO frequency-selective channels, and derive the sufficient conditions on the number of required RF chains at the ET so that hybrid beamforming is able to achieve the same optimal performance as the fully digital beamforming, regardless of the number of antenna elements at the ET or ER. Specifically, for LoS environment, we show that only one RF chain is required to achieve the optimal fully digital beamforming performance. For the case of general multi-path channels, we show that the number of RF chains is sufficient if it is no less than twice the number of used sub-bands or twice the number of channel paths. Moreover, for the special case of multiple-input single-output (MISO) WPT system with single antenna at the ER, the required number of RF chains can be further reduced to the same as the number of channel paths only. The corresponding optimal hybrid analog/digital beamforming design in each scenario is also provided in our constructive proof given in the appendices. Note that the obtained results are of high practical value for WPT systems, as it provides a theoretical guidance on the number of RF chains required to achieve the same performance as the fully digital beamforming for any given system configuration. Moreover, our result also implies that given the WPT environment (e.g., the number of channel paths), the performance of WPT systems can be enhanced by increasing the number of antennas at the ET/ER, yet without the need of increasing the RF chain cost at the ET, which thus provides important design insight for practical implementations.

Next, for the scenarios when the number of RF chains is insufficient to achieve the fully digital beamforming performance, we propose two algorithms for the hybrid analog/digital beamforming design to approach the optimal performance. Motivated by the results for the optimal hybrid beamforming design with sufficient number of RF chains, the proposed algorithms are based on the principle of matching the analog beamforming matrix with the eigen-directions of different frequency sub-channels to the best effort, by following two different matching criteria. Simulation results show that the performances of the proposed algorithms improve with the number of available RF chains, and they eventually converge

This article has been accepted for publication in a future issue of this journal, but has not been fully edited. Content may change prior to final publication. Citation information: DOI 10.1109/TWC.2018.2865313, IEEE Transactions on Wireless Communications

to the fully digital beamforming performance as the number RF chains becomes sufficiently large as derived for the optimal hybrid beamforming.

The rest of this paper is organized as follows. Section II presents the system model for MIMO WPT over general frequency-selective channels. In Section III, the optimal design for fully digital MIMO WPT is reviewed. In Section IV, we present the WPT architecture with hybrid analog/digital beamforming and its design problem formulation. In Section V, we show the sufficient conditions on the number of RF chains for hybrid beamforming to achieve the optimal performance as the fully digital beamforming. In Section VI, we present efficient algorithms for the hybrid beamforming design in the case of insufficient number of RF chains. Numerical results are given in Section VII to verify the performance of the proposed designs in various scenarios. Finally, Section VIII concludes the paper.

Notations: In this paper, boldface lower- and upper-case letters denote vectors and matrices, respectively. $\mathbb{C}^{M\times N}$ denotes the space of $M\times N$ complex-valued matrices. For a vector $\mathbf{a}$, $(\mathbf{a})_l$ denotes its lth element. For a matrix $\mathbf{A}$, its inverse, transpose, Hermitian transpose, trace, and rank are respectively denoted as $\mathbf{A}^{-1}$, $\mathbf{A}^T$, $\mathbf{A}^H$, $\mathrm{tr}(\mathbf{A})$ and $\mathrm{rank}(\mathbf{A})$. The ith column of matrix $\mathbf{A}$ is denoted by the lower-case letter $\mathbf{a}^i$, and $\mathbf{A}^{i:j}$ denotes a sub-matrix of $\mathbf{A}$ containing its ith column to the jth column. For a square matrix $\mathbf{A}$, $(\mathbf{A})_{l,l}$ denotes its lth diagonal element, and $\mathbf{A}\succeq\mathbf{0}$ denotes that A is a positive semi-definite matrix. Moreover, $\mathrm{diag}(x_1,\cdots,x_M)$ denotes an $M\times M$ diagonal matrix with $x_1\cdots x_M$ being the diagonal elements. $\delta(t)$ denotes the Dirac delta function. $\Re\{c\}$ denotes the real part of a complex number c, and the symbol j represents the imaginary unit of complex numbers, i.e., $j^2=-1$. $\mathbb{E}[\cdot]$ represents the expectation operator. $\angle(\cdot)$ represents the phase angle operator. For a real number a, $\lfloor a\rfloor$ and $\lceil a\rceil$ denote the largest integer no greater than a and the smallest integer no less than a, respectively. Furthermore, $\mathcal{CN}(\boldsymbol{\mu},\mathbf{C})$ denotes the circularly symmetric complex Gaussian (CSCG) distribution of a random vector with mean $\boldsymbol{\mu}$ and covariance matrix $\mathbf{C}$.

II. System Model

We consider a point-to-point MIMO WPT system, where an ET with $M_{\mathrm{T}}>1$ transmit antennas sends power wirelessly via RF transmission to an ER with $M_{\mathrm{R}}\geq 1$ receive antennas. We adopt a geometric channel model with L scatterers, and each scatterer is assumed to contribute one (significant) propagation path between the ET and the ER [33], [34]. Furthermore, we assume that the channel is quasi-static, i.e., it remains constant over each transmission block with a certain duration and may vary from one block to another. Under this channel model, in each block, the channel impulse response from the ET to the ER can be expressed as

$$\mathbf{H}(t)=\sum_{l=1}^{L}\alpha_l\mathbf{a}(\varphi_l^r,\theta_l^r)\mathbf{b}^H(\varphi_l^t,\theta_l^t)\delta(t-\tau_l), \tag{1}$$

where L denotes the number of channel paths between the ET and the ER, α_l and τ_l denote the complex gain and delay (in second) of the lth path, respectively. Specifically, α_l is modeled as $\alpha_l=\sqrt{\beta\kappa_l}e^{j\eta_l}$, where $\beta>0$ denotes the large-scale path loss, $\kappa_l>0$ and $\eta_l\sim[0,2\pi]$ denote the fractional power ratio and phase shift of the lth path, respectively, with $\sum_{l=1}^{L}\kappa_l=1$. Furthermore, φ_l^r and θ_l^r denote its azimuth and elevation angle of arrival (AoA) at the ER, respectively, and φ_l^t and θ_l^t denote its azimuth and elevation angle of departure (AoD) at the ET, respectively. Without loss of generality, we assume that $\tau_1=0$ and $\tau_1\leq\tau_2\cdots\leq\tau_L$. In addition, $\mathbf{a}(\cdot)$ and $\mathbf{b}(\cdot)$ represent the receive and transmit array response vectors at the ER and ET as a function of the AoA and AoD, respectively. For typical antenna arrays, each element in the array response vector for a given signal path constitutes the relative phase shift of the corresponding array element with respect to a reference one. For instance, assuming that an uniform planar array (UPA) is equipped at the ET with Y and Z antenna elements on the y and z axes, respectively, the array response at the ET can be written as [39]

$$\mathbf{b}(\varphi_l^t,\theta_l^t)=\sqrt{\frac{1}{M_{\mathrm{T}}}}\Big[1,\cdots,e^{j\frac{2\pi}{\lambda}d(m\sin(\varphi_l^t)\cos(\theta_l^t)+w\sin(\theta_l^t))},\cdots,e^{j\frac{2\pi}{\lambda}d((Y-1)\sin(\varphi_l^t)\cos(\theta_l^t)+(Z-1)\sin(\theta_l^t))}\Big]^T, \tag{2}$$

for $l=1,\cdots,L$, where λ denotes the signal wavelength, d denotes the inter-element spacing, $0\leq m\leq Y-1$ and $0\leq w\leq Z-1$ denote the y and z indices of an antenna element, respectively, and $M_{\mathrm{T}}=YZ$ is the total number of array elements.

We assume that the total available bandwidth for the WPT system is B in Hz, where $B\tau_L>1$, so that the channel is in general frequency-selective. The total bandwidth B is equally partitioned into N orthogonal sub-bands each of bandwidth $B_s=B/N$, where N is properly chosen so that the channel in each sub-band is approximately frequency-flat. It follows from (1) that the resulting MIMO channel matrix of sub-band n can be expressed as [40], [41]

$$\mathbf{H}_n=\sum_{l=1}^{L}\alpha_{ln}\mathbf{a}(\varphi_l^r,\theta_l^r)\mathbf{b}^H(\varphi_l^t,\theta_l^t),n=1,\cdots,N, \tag{3}$$

where $\alpha_{ln}=\alpha_l e^{-j2\pi\frac{nB\tau_l}{N}}$ denotes the complex gain of the lth path at sub-band n. As a preliminary study on hybrid beamforming for WPT systems, in this paper, we assume that the channel frequency response of all sub-bands, $\{\mathbf{H}_n\}$, are perfectly known at the ET, for the purpose of investigating the performance limits of hybrid beamfoming for WPT.

Note that we have assumed that the AoA and AoD of each path remains the same in different sub-bands. This is practically valid since in a typical transmission environment, the propagation characteristics of obstacles mainly depend on their permittivities and conductivities, which have little frequency dependence within a finite bandwidth [42].

The transmitted signal at antenna m, $m=1,\cdots,M_{\mathrm{T}}$, can

This article has been accepted for publication in a future issue of this journal, but has not been fully edited. Content may change prior to final publication. Citation information: DOI 10.1109/TWC.2018.2865313, IEEE Transactions on Wireless Communications

be expressed as

$$\begin{aligned} x_m(t) &= \sum_{n=1}^{N} \sqrt{2a_{mn}(t)}\cos(2\pi f_n t + \phi_{mn}(t)) \\ &= \sqrt{2}\Re\left\{\sum_{n=1}^{N} s_{mn}(t)e^{j2\pi f_n t}\right\}, \end{aligned} \tag{4}$$

where f_n is the carrier frequency at the nth sub-band, $s_{mn}(t) = a_{mn}(t)e^{j\phi_{mn}(t)}$ represents the equivalent baseband signal sent by antenna m over the sub-band n, and $\mathbf{s}_n(t) \triangleq [s_{1n}(t), \cdots, s_{M_{\rm T}n}(t)]^T$ denotes the signals transmitted by the $M_{\rm T}$ antennas of the ET over sub-band n.

The total received RF power at the ER can be expressed as

$$Q = \sum_{n=1}^{N} \mathrm{tr}(\mathbf{H}_n \mathbf{S}_n \mathbf{H}_n^H), \tag{5}$$

where $\mathbf{S}_n \triangleq \mathbb{E}[\mathbf{s}_n(t)\mathbf{s}_n(t)^H] \in \mathbb{C}^{M_{\rm T}\times M_{\rm T}}$ denotes the transmit covariance matrix at sub-band n. Note that in this paper, we focus on maximizing the received total RF power at the ER. This is equivalent to maximizing the total harvested DC power at the ER if the linear energy harvesting model is assumed, where the harvested DC power is linearly proportional to Q [2]. However, for practical energy harvesting model which is non-linear [2], [43], [44], maximizing the RF power Q in general does not yield the maximum harvested DC power, while it is still essential to maximize the end-to-end WPT efficiency which is practically bottlenecked by the severe RF power attenuation in wireless transmission. Note that in general $\mathbf{s}_n(t)$ may constitute pseudo-random signals. For the special case of unmodulated WPT with $s_{mn}(t)$ being deterministic, we have $\mathbf{S}_n = \mathbf{s}_n\mathbf{s}_n^H$, $\forall n$, which is constrained to be a rank-one matrix.

III. MIMO WPT with Fully Digital Beamforming

In this section, we give a brief overview on the optimal energy beamforming design for the fully digital beamforming architecture, which can be used as a benchmark for our subsequent study of the hybrid beamforming. For WPT systems with fully digital beamforming, each transmit antenna at the ET is connected to one dedicated RF chain so that both the amplitudes and phases of the transmitted signals from all antennas can be flexibly adjusted based on the channel realization. As a result, there is no additional constraint on the structure of the transmit covariance matrix $\mathbf{S}_n$ at each sub-band, except that it should be a positive semi-definite matrix. Therefore, the power maximization problem of fully digital beamforming can be formulated as [2]

$$\begin{aligned} (\mathrm{P1}): \ \underset{\{\mathbf{S}_n\}}{\mathrm{Max.}} \quad & \sum_{n=1}^{N} \mathrm{tr}(\mathbf{H}_n \mathbf{S}_n \mathbf{H}_n^H), \\ \text{s. t.} \quad & \mathrm{tr}(\mathbf{S}_n) \le P_s, \forall n, \\ & \sum_{n=1}^{N} \mathrm{tr}(\mathbf{S}_n) \le P_t, \\ & \mathbf{S}_n \succeq \mathbf{0}, \forall n, \end{aligned}$$

where $\mathrm{tr}(\mathbf{S}_n)$ denotes the transmitted power at sub-band n, P_t denotes the maximum transmission power at the ET across all sub-bands, and $P_s = P_0\frac{B}{N}$ denotes the maximum transmit power constraint at each frequency sub-band, with P_0 being the average power spectrum density (PSD) constraint in Watt per Hertz (W/Hz), which could correspond to the constraint imposed by the regulatory authorities [45]. For convenience, we assume that P_t is an integer multiple of P_s, i.e., $P_t/P_s = N'$ for some integer $1 \le N' \le N$.

The problem (P1) has been optimally solved in [2]. Specifically, the received power in each sub-band can be maximized by transmitting one single beam, with the beamforming vector designed as the eigenvector corresponding to the dominant eigenvalue of the channel matrix [7], i.e.,

$$\mathbf{S}_n = p_n \mathbf{v}_n^*(\mathbf{v}_n^*)^H, n = 1, \cdots, N, \tag{6}$$

where $\mathbf{v}_n^* = \mathbf{v}_{\max}(\mathbf{H}_n^H\mathbf{H}_n)$ denotes the eigenvector corresponding to the largest eigenvalue of the matrix $\mathbf{H}_n^H\mathbf{H}_n$ at sub-band n, and $p_n = \mathrm{tr}(\mathbf{S}_n)$ denotes the transmit power allocated to sub-band n. Furthermore, it is optimal to allocate the power to those N' strongest sub-bands with the N' largest eigenvalues [2], i.e.,

$$p_{[n]} = \begin{cases} P_s, & n = 1, \cdots, N' \\ 0, & n = N'+1, \cdots, N, \end{cases} \tag{7}$$

where $[\cdot]$ is the permutation over all the N sub-bands such that $\lambda_{\max,[1]} \ge \cdots \ge \lambda_{\max,[N]}$, with $\lambda_{\max,n}$ denoting the maximum eigenvalue of the matrix $\mathbf{H}_n^H\mathbf{H}_n$. As a result, the maximum received power with fully digital energy beamforming is given by

$$Q^*_{\rm digital} = P_s \sum_{n=1}^{N'} \lambda_{\max,[n]}. \tag{8}$$

The result in (6) shows that for each sub-band, $\mathbf{S}_n$ is a rank-one matrix, which means that unmodulated transmission is optimal, i.e., the baseband equivalent transmitted signal $\mathbf{s}_n(t)$ at each sub-band is time-invariant, which is given by

$$\mathbf{s}_n = \sqrt{p_n}\mathbf{v}_n^*, \ n = 1, \cdots, N. \tag{9}$$

IV. MIMO WPT with Hybrid Beamforming

The fully digital MIMO WPT systems incur prohibitively high RF chain cost at the ET when the number of transmit antennas $M_{\rm T}$ becomes very large. To achieve cost-effective power transmission, we consider a practical WPT system with $M_{\rm RF} \le M_{\rm T}$ RF chains available at the ET and the new hybrid analog/digital beamforming architecture is adopted. With this architecture, the limited RF chains are connected with a larger number of antenna elements via power splitters followed by a network of analog phase shifters, as shown in Fig. 1. At each of the selected sub-band n, the ET first applies a baseband digital beamformer of size $M_{\rm RF} \times K_n$, with K_n denoting the number of digital beams at sub-band n, followed by an analog beamformer of size $M_{\rm T} \times M_{\rm RF}$ that is common for all sub-bands and implemented with analog phase shifters.

Denote by $\mathbf{F}_{{\rm BB},n} \in \mathbb{C}^{M_{\rm RF}\times K_n}$ the baseband digital beamformer at sub-band n, and $\mathbf{d}_n(t) \in \mathbb{C}^{K_n\times 1}$ with

This article has been accepted for publication in a future issue of this journal, but has not been fully edited. Content may change prior to final publication. Citation information: DOI 10.1109/TWC.2018.2865313, IEEE Transactions on Wireless Communications

$\mathbb{E}[\mathbf{d}_n(t)\mathbf{d}_n(t)^H] = \frac{1}{K_n}\mathbf{I}$ the pseudo-random energy signal sent at this sub-band. The signal transmitted by the $M_{\rm T}$ antennas of the ET over sub-band n is thus given by

$$\mathbf{s}_n(t) = \sqrt{p_n}\mathbf{F}_{\rm RF}\mathbf{F}_{{\rm BB},n}\mathbf{d}_n(t), \tag{10}$$

where p_n denotes the transmit power at sub-band n, and $\mathbf{F}_{\rm RF} \in \mathbb{C}^{M_{\rm T}\times M_{\rm RF}}$ denotes the analog beamformer implemented using phase shifters, whose elements are constrained to all have identical magnitude, i.e.,

$$(\mathbf{f}_{\rm RF}^i(\mathbf{f}_{\rm RF}^i)^H)_{l,l} = \frac{1}{M_{\rm T}},\ i = 1,\cdots,M_{\rm RF},\ l = 1,\cdots,M_{\rm T}. \tag{11}$$

Accordingly, the transmit covariance matrix at sub-band n can be written as

$$\begin{aligned}\mathbf{S}_n &= \mathbb{E}[\mathbf{s}_n(t)\mathbf{s}_n(t)^H] \\ &= \frac{p_n}{K_n}\mathbf{F}_{\rm RF}\mathbf{F}_{{\rm BB},n}\mathbf{F}_{{\rm BB},n}^H\mathbf{F}_{\rm RF}^H,\ n = 1,\cdots,N.\end{aligned} \tag{12}$$

To ensure that the transmit power at sub-band n is given by $\mathrm{tr}(\mathbf{S}_n) = p_n$, we have the following constraint on the digital and analog beamformers,

$$\mathrm{tr}(\mathbf{F}_{\rm RF}\mathbf{F}_{{\rm BB},n}\mathbf{F}_{{\rm BB},n}^H\mathbf{F}_{\rm RF}^H) = K_n,\ n = 1,\cdots,N. \tag{13}$$

It then follows from (5) and (12) that the received RF power at the ER with hybrid beamforming can be expressed as

$$Q_{\rm hybrid} = \sum_{n=1}^{N}\frac{p_n}{K_n}\mathrm{tr}(\mathbf{H}_n\mathbf{F}_{\rm RF}\mathbf{F}_{{\rm BB},n}\mathbf{F}_{{\rm BB},n}^H\mathbf{F}_{\rm RF}^H\mathbf{H}_n^H), \tag{14}$$

and the corresponding power maximization problem can be formulated as

$$\begin{aligned}(\mathrm{P2}):\ \max_{\mathbf{F}_{\rm RF},\{\mathbf{F}_{{\rm BB},n},p_n\}}\ & Q_{\rm hybrid} \\ \text{s.t.}\ & (11),(13), \\ & 0 \le p_n \le P_s, \forall n, \\ & \sum_{n=1}^{N} p_n \le P_t.\end{aligned}$$

Problem (P2) is non-convex due to the non-concave objective function and the non-convex constant-modulus constraint on the elements of $\mathbf{F}_{\rm RF}$. Thus, it is in general difficult to be optimally solved efficiently. To tackle this problem, we first provide the following lemma.

Lemma 1. For any given analog beamformming design $\mathbf{F}_{\rm RF}$, the optimal digital beamforming $\mathbf{F}_{{\rm BB},n}$ to (P2) can be expressed as

$$\mathbf{F}_{{\rm BB},n} = (\mathbf{F}_{\rm RF}^H\mathbf{F}_{\rm RF})^{-\frac{1}{2}}\hat{\mathbf{v}}_n^*,\ n = 1,\cdots,N, \tag{15}$$

where $\hat{\mathbf{v}}_n^*$ denotes the eigenvector corresponding to the dominant eigenvalue of $\mathbf{H}_{eq,n}^H\mathbf{H}_{eq,n}$, with $\mathbf{H}_{eq,n} = \mathbf{H}_n\mathbf{F}_{\rm RF}(\mathbf{F}_{\rm RF}^H\mathbf{F}_{\rm RF})^{-\frac{1}{2}}$ denoting the equivalent channel matrix at sub-band n.

Proof. Please refer to Appendix A. □

Lemma 1 shows that for MIMO WPT with hybrid beamforming, the optimal digital beamforming of each sub-band is always a vector, i.e., it is optimal to transmit only one single beam at each sub-band so that $K_n = 1$, $\forall n$. Hence, in the following, $\mathbf{F}_{{\rm BB},n}$ is re-labeled as $\mathbf{f}_{{\rm BB},n} \in \mathbb{C}^{M_{\rm RF}\times 1}$ for representing the baseband digital beamforming vector at sub-band n.

As a result, problem (P2) can be re-written as

$$\begin{aligned}(\mathrm{P2}'):\ \max_{\mathbf{F}_{\rm RF},\{\mathbf{f}_{{\rm BB},n},p_n\}}\ & \sum_{n=1}^{N} p_n\mathrm{tr}(\mathbf{H}_n\mathbf{F}_{\rm RF}\mathbf{f}_{{\rm BB},n}\mathbf{f}_{{\rm BB},n}^H\mathbf{F}_{\rm RF}^H\mathbf{H}_n^H) \\ \text{s.t.}\ & (11), \\ & \mathrm{tr}(\mathbf{F}_{\rm RF}\mathbf{f}_{{\rm BB},n}\mathbf{f}_{{\rm BB},n}^H\mathbf{F}_{\rm RF}^H) = 1, \forall n, \\ & p_n \le P_s, \forall n, \\ & \sum_{n=1}^{N} p_n \le P_t.\end{aligned}$$

Note that for any optimal solution $\mathbf{F}_{\rm RF}$ and $\{\mathbf{f}_{{\rm BB},n}, p_n\}$ to problem (P2′), we can obtain a feasible solution to the fully digital beamforming problem (P1) that achieves the same objective value by letting $\mathbf{S}_n = p_n\mathbf{f}_{{\rm hybrid},n}\mathbf{f}_{{\rm hybrid},n}^H$, with $\mathbf{f}_{{\rm hybrid},n} = \mathbf{F}_{\rm RF}\mathbf{f}_{{\rm BB},n}$, $n = 1,\cdots,N$. This implies that the maximum received power with hybrid beamforming, denoted as $Q_{\rm hybrid}^*$, cannot be larger than that with fully digital beamforming, $Q_{\rm digital}^*$, i.e.,

$$Q_{\rm hybrid}^* \le Q_{\rm digital}^*. \tag{16}$$

Furthermore, we have the following proposition.

Proposition 1. A sufficient condition for (16) to hold with equality is that there exists a set of analog and digital beamformers $\mathbf{F}_{\rm RF}$ and $\{\mathbf{f}_{{\rm BB},n}\}$ that realize the optimal fully digital beamformer at all the N' strongest sub-bands, i.e.,

$$\mathbf{F}_{\rm RF}\mathbf{f}_{{\rm BB},[n]} = \mathbf{v}_{[n]}^*, n = 1,\cdots,N', \tag{17}$$

where $\mathbf{v}_n^*$ is defined below equation (6).

Note that from Proposition 1, it follows that if the number of RF chains is the same as the number of antennas, i.e., $M_{\rm RF} = M_{\rm T}$, $\mathbf{F}_{\rm RF}$ becomes a square matrix, and the condition in (17) can be satisfied by setting $\mathbf{F}_{\rm RF}$ as the unitary Discrete Fourier Transform (DFT) matrix and $\mathbf{f}_{{\rm BB},[n]} = \mathbf{F}_{\rm RF}^{-1}\mathbf{v}_n^*$, $\forall n$. In the next section, we aim to answer the following question: for $M_{\rm RF} < M_{\rm T}$, how many RF chains are needed to achieve (17) so that the hybrid beamforming gives the optimal performance as the fully digital beamforming?

V. Number of RF chains for Hybrid Beamforming to Achieve Fully Digital Performance

To gain some insight, we first consider the special case of LoS channels, where the number of channel paths in (1) is $L = 1$.

Proposition 2. For MIMO WPT over LoS channels, the optimal fully digital beamforming performance can be achieved with one single RF chain at the ET, i.e., $M_{\rm RF} = 1$.

Proof. Please refer to the constructive proof in Appendix B. □

Proposition 2 indicates that for the special case of LoS channel, one RF chain is sufficient to achieve the optimal

This article has been accepted for publication in a future issue of this journal, but has not been fully edited. Content may change prior to final publication. Citation information: DOI 10.1109/TWC.2018.2865313, IEEE Transactions on Wireless Communications

performance for MIMO WPT systems, regardless of the number of antenna elements $M_{\rm T}$ and that of the used sub-bands N'. This result is due to the fact that for the LoS channel with only one signal path, the optimal beamforming at the ET only needs to align with one AoD of the path, which can be achieved by merely adjusting the phases at different antennas, without requiring the amplitude variation across them. Thus, analog beamforming suffices and no digital beamforming is needed.

Next, we consider another special case with only one single antenna at the ER or MISO WPT system.

Proposition 3. For MISO WPT with $M_{\rm R} = 1$, the optimal fully digital beamforming performance can be achieved if the number of RF chains at the ET is no less than the number of channel paths, i.e., $M_{\rm RF} \geq L$.

Proof. Please refer to the constructive proof in Appendix C. □

In the following, we study the most general setup of MIMO WPT in multi-path channels. To this end, we first introduce the following proposition.

Proposition 4. For MIMO WPT over multi-path channels, the optimal fully digital beamforming performance can be achieved if the number of RF chains at the ET is no less than twice the rank of $\mathbf{V} \triangleq \left[\begin{array}{ccc} \mathbf{v}_{[1]}^* & \cdots & \mathbf{v}_{[N']}^* \end{array}\right] \in \mathbb{C}^{M_{\rm T}\times N'}$, i.e., $M_{\rm RF} \geq 2 \cdot {\rm rank}(\mathbf{V})$, where $\mathbf{v}_{[n]}^*$ is defined below (6).

Proof. Please refer to the constructive proof in Appendix D. □

Furthermore, we have the following lemma.

Lemma 2. The rank of $\mathbf{V} \in \mathbb{C}^{M_{\rm T}\times N'}$ is no larger than N' or the number of multi-path L, i.e., ${\rm rank}(\mathbf{V}) \leq \min\{L, N'\}$.

Proof. Please refer to Appendix E. □

By combining Proposition 4 and Lemma 2, the following sufficient conditions can be obtained on the number of required RF chains to achieve fully digital WPT performance for the general MIMO WPT systems over multi-path channels.

Theorem 1. For MIMO WPT using N' sub-bands over a multi-path channel with L paths, the fully digital WPT performance can be achieved if $M_{\rm RF} \geq \min\{2L, 2N'\}$.

Moreover, for the special MISO WPT system, a more relaxed sufficient condition can be obtained in the following corollary by combining Proposition 3 and Theorem 1.

Corollary 1. For MISO WPT using N' sub-bands over a multi-path channel with L paths, the fully digital WPT performance can be achieved if $M_{\rm RF} \geq \min\{L, 2N'\}$.

Theorem 1 and Corollary 1 show that fully digital WPT performance can be achieved in general with a smaller number of RF chains than $M_{\rm T}$ at the ET when either one of the following two conditions holds. The first condition is when N' is sufficiently small, i.e., $N' < M_{\rm T}/2$, which may correspond to the scenarios of narrow bandwidth and/or loose power spectrum density constraint (with higher P_s). For instance, for narrow-band multi-path channel with $N = N' = 1$, only two RF chains are needed for hybrid beamforming to achieve fully digital WPT performance based on Theorem 1. This is consistent with the similar result for narrow-band wireless communications with hybrid analog/digital precoding, i.e., two RF chains are needed to achieve fully digital communication performance if only one data stream is transmitted [29], [32]. The second condition applies when the number of channel paths L is sufficiently small (i.e., $L < M_{\rm T}/2$ for MIMO WPT or $L < M_{\rm T}$ for MISO WPT), which may occur in e.g., millimeter wave based systems with small numbers of channel multi-path [46].

For many practical systems with the number of RF chains $M_{\rm RF}$ given, the above sufficient conditions to achieve optimal digital beamforming performance may not hold. In this case, the hybrid analog/digital beamformers need to be jointly designed to approach the optimal fully digital beamforming performance, as will be pursued in the next section.

VI. Hybrid Beamforming Design with Insufficient RF Chains

When the number of RF chains at the ET is insufficient to achieve the optimal digital beamforming performance, problem (P2′) is difficult to be optimally solved in general. In this case, we aim to design efficient hybrid beamforming algorithms to maximize the WPT performance.

To this end, we first adopt the same set of selected sub-bands and their transmit power allocation as for the fully digital case in (7). As a result, problem (P2′) reduces to

$$\begin{aligned}(\text{P3}): \max_{\mathbf{F}_{\rm RF}, \{\mathbf{f}_{{\rm BB},[n]}\}} \quad & P_s \sum_{n=1}^{N'} {\rm tr}(\mathbf{H}_{[n]}\mathbf{F}_{\rm RF}\mathbf{f}_{{\rm BB},[n]}\mathbf{f}_{{\rm BB},[n]}^H\mathbf{F}_{\rm RF}^H\mathbf{H}_{[n]}^H) \\ \text{s.t.} \quad & (11), \\ & {\rm tr}(\mathbf{F}_{\rm RF}\mathbf{f}_{{\rm BB},[n]}\mathbf{f}_{{\rm BB},[n]}^H\mathbf{F}_{\rm RF}^H) = 1,\end{aligned}$$

The main difficulty of optimally solving (P3) lies in the fact that the analog and digital beamforming variables $\mathbf{F}_{\rm RF}$ and $\mathbf{f}_{{\rm BB},[n]}$ are closely coupled in the objective function as well as the power constraint. Fortunately, for any given $\mathbf{F}_{\rm RF}$, the optimal digital beamformers $\mathbf{f}_{{\rm BB},[n]}$ can be obtained based on (15). Thus, solving problem (P3) reduces to finding the analog beamforming design $\mathbf{F}_{\rm RF}$. In the following, motivated by the results obtained in Section V, we propose two efficient algorithms for the design of the analog beamformers $\mathbf{F}_{\rm RF}$.

Recall that according to Proposition 4 and its constructive proof in Appendix D, with sufficient number of RF chains at the ET, the optimal analog beamforming matrix $\mathbf{F}_{\rm RF}$ is designed to completely span the left singular space of $\mathbf{V}$, where $\mathbf{V} \triangleq \left[\begin{array}{ccc} \mathbf{v}_{[1]}^* & \cdots & \mathbf{v}_{[N']}^* \end{array}\right]$ and its (reduced) singular value decomposition (SVD) is given by $\mathbf{V} = \mathbf{U}\mathbf{\Gamma}\mathbf{W}^H$. In this case, each column of $\mathbf{U}$ can be represented by a linear combination of the columns in $\mathbf{F}_{\rm RF}$.

Therefore, when the number of RF chains is insufficient, one viable approach is to design $\mathbf{F}_{\rm RF}$ to partially span the left singular space of $\mathbf{V}$. To this end, we first introduce the matrix $\bar{\mathbf{V}} = \mathbf{V}\cdot{\rm diag}(\lambda_{{\rm max},[1]}, \cdots, \lambda_{{\rm max},[N']})$ by incorporating the weighting factors $\{\lambda_{{\rm max},[n]}\}$ of the selected sub-bands. Furthermore, let the SVD of $\bar{\mathbf{V}}$ be expressed as $\bar{\mathbf{V}} = \bar{\mathbf{U}}\bar{\mathbf{\Gamma}}\bar{\mathbf{W}}^H$, where $r = {\rm rank}(\bar{\mathbf{V}})$, $\bar{\mathbf{U}} \in \mathbb{C}^{M_{\rm T}\times r}$ and $\bar{\mathbf{W}} \in \mathbb{C}^{N'\times r}$ contain

This article has been accepted for publication in a future issue of this journal, but has not been fully edited. Content may change prior to final publication. Citation information: DOI 10.1109/TWC.2018.2865313, IEEE Transactions on Wireless Communications

the left and right singular vectors of $\bar{\mathbf{V}}$, respectively, and $\bar{\mathbf{\Gamma}} = \mathrm{diag}(\bar{\gamma}_1, \cdots, \bar{\gamma}_r)$ with $\bar{\gamma}_1 \geq \cdots \geq \bar{\gamma}_r$ contains the ordered singular values.

In the following, the columns of $\mathbf{F}_{\mathrm{RF}}$ are designed such that they span $\bar{\mathbf{U}}$ to the best efforts using two different approaches, based on which two efficient algorithms are then proposed for the design of the analog beamforming matrix $\mathbf{F}_{\mathrm{RF}}$.

A. Two Approaches to Design Columns in $\mathbf{F}_{\mathrm{RF}}$

1) Column Design Approach 1: In the first approach, we design one pair of columns in $\mathbf{F}_{\mathrm{RF}}$, say $\mathbf{f}_{\mathrm{RF}}^{i}$ and $\mathbf{f}_{\mathrm{RF}}^{i+1}$, $i \in \{1, \cdots, M_{\mathrm{RF}}-1\}$, based on one corresponding column in $\bar{\mathbf{U}}$, say $\bar{\mathbf{u}}^j$, $j \in \{1, \cdots, r\}$, such that $\bar{\mathbf{u}}^j$ can be represented by a linear combination of $\mathbf{f}_{\mathrm{RF}}^{i}$ and $\mathbf{f}_{\mathrm{RF}}^{i+1}$. This can be achieved by following the constructive proof of Proposition 4 in Appendix D.

2) Column Design Approach 2: In the second approach, we design each column of $\mathbf{F}_{\mathrm{RF}}$, say $\mathbf{f}_{\mathrm{RF}}^{i}$, $i \in \{1, \cdots, M_{\mathrm{RF}}\}$, based on one corresponding column in $\bar{\mathbf{U}}$, say $\bar{\mathbf{u}}^j$, $j \in \{1, \cdots, r\}$, such that its projection on $\bar{\mathbf{u}}^j$ is maximized, i.e.,

$$\begin{aligned} \underset{\mathbf{f}_{\mathrm{RF}}^{i}}{\text{Max.}} \quad & |(\mathbf{f}_{\mathrm{RF}}^{i})^H \bar{\mathbf{u}}^j|^2 \\ \text{s. t.} \quad & (\mathbf{f}_{\mathrm{RF}}^{i}(\mathbf{f}_{\mathrm{RF}}^{i})^H)_{l,l} = \frac{1}{M_{\mathrm{T}}},\ l = 1 \cdots, M_{\mathrm{T}}. \end{aligned} \tag{18}$$

The optimal solution of (18) can be obtained in closed-form [47], which is given by

$$(\mathbf{f}_{\mathrm{RF}}^{i})_l = \frac{1}{\sqrt{M_{\mathrm{T}}}} e^{j\angle(\bar{\mathbf{u}}^j)_l},\ l = 1, \cdots, M_{\mathrm{T}}. \tag{19}$$

Algorithm 1 Proposed Analog Beamforming Scheme 1

Input: $\mathbf{H}_{[n]}$, $n = 1, \cdots, N'$
Output: $\mathbf{F}_{\mathrm{RF}}$
1: Calculate $\mathbf{V}$, $\bar{\mathbf{V}}$, and $\bar{\mathbf{U}}$.
2: **for** $i = 1 \rightarrow K$ **do**
3: Design $\mathbf{f}_{\mathrm{RF}}^{2i-1}$ and $\mathbf{f}_{\mathrm{RF}}^{2i}$ based on $\bar{\mathbf{u}}^i$ using column design approach 1.
4: **end for**
5: **if** M_{RF} is odd **then**
6: Design $\mathbf{f}_{\mathrm{RF}}^{M_{\mathrm{RF}}}$ based on $\bar{\mathbf{u}}^{K+1}$ using column design approach 2.
7: **end if**

B. Proposed Analog Beamforming Schemes

Following the two column design approaches in the preceding subsection, we propose two corresponding schemes to design the analog beamforming matrix $\mathbf{F}_{\mathrm{RF}}$ in the following, respectively. The first scheme mainly uses the column design approach 1, whereas the second scheme gives higher priority to column design approach 2.

1) Analog Beamforming Scheme 1: Let $K = \lfloor \frac{M_{\mathrm{RF}}}{2} \rfloor$. In this scheme, $\mathbf{F}_{\mathrm{RF}}$ is designed such that it spans the K most dominant eigen-directions of $\bar{\mathbf{V}}$, i.e., the first K columns of $\bar{\mathbf{U}}$. To this end, the $(2i-1)$th and $(2i)$th columns of $\mathbf{F}_{\mathrm{RF}}$ are designed based on the ith column of $\bar{\mathbf{U}}$, $i = 1, \cdots, K$, via the column design approach 1. If M_{RF} is an odd number, the $(2K+1)$th (last) column of $\mathbf{F}_{\mathrm{RF}}$ is designed based on the $(K+1)$th column of $\bar{\mathbf{U}}$ using column design approach 2.

Hence, the above scheme for the design of $\mathbf{F}_{\mathrm{RF}}$ is summarized in Algorithm 1.

Note that this analog beamforming scheme mainly utilizes column design approach 1. With this scheme, the $K = \lfloor \frac{M_{\mathrm{RF}}}{2} \rfloor$ most dominant eigen-directions of $\bar{\mathbf{V}}$ are spanned by the columns of $\mathbf{F}_{\mathrm{RF}}$, whereas the remaining $(r-K)$ (or $(r-K-1)$ if M_{RF} is odd) eigen-directions are ignored in the design of $\mathbf{F}_{\mathrm{RF}}$. This is desirable if M_{RF} is relatively large, but could be inefficient when M_{RF} is small, as some significant eigen-directions have to be ignored. Hence, in the following, we propose an alternative scheme that includes more eigen-directions in general.

2) Analog Beamforming Scheme 2: In this scheme, higher priority is given to include as many eigen-directions as possible in the design of $\mathbf{F}_{\mathrm{RF}}$, even though they cannot be completely spanned by $\mathbf{F}_{\mathrm{RF}}$. Specifically, if $M_{\mathrm{RF}} \leq r$, where r is the number of columns in $\bar{\mathbf{U}}$, each column of $\mathbf{F}_{\mathrm{RF}}$ is designed based on one corresponding column in $\bar{\mathbf{U}}$ using column design approach 2. Therefore, in total M_{RF} eigen-directions of $\bar{\mathbf{V}}$ are considered in the design. On the other hand, if $M_{\mathrm{RF}} > r$, the number of RF chains is large enough to include all eigen-directions in the design. As a result, the extra design degrees-of-freedom (DoF) can then be used for the most dominant eigen-directions such that they are completely spanned by $\mathbf{F}_{\mathrm{RF}}$. Specifically, let $s = M_{\mathrm{RF}} - r$, we design the first $2s$ columns of $\mathbf{F}_{\mathrm{RF}}$ based on the first s columns of $\bar{\mathbf{U}}$ using column design approach 1, as in Algorithm 1. Then, each of the last $(r-s)$ columns of $\mathbf{F}_{\mathrm{RF}}$ is designed based on one of the remaining $(r-s)$ columns of $\bar{\mathbf{U}}$ using column design approach 2. The above scheme is summarized in Algorithm 2.

This article has been accepted for publication in a future issue of this journal, but has not been fully edited. Content may change prior to final publication. Citation information: DOI 10.1109/TWC.2018.2865313, IEEE Transactions on Wireless Communications

Algorithm 2 Proposed Analog Beamforming Scheme 2

Input: $\mathbf{H}_{[n]}$, $n = 1, \cdots, N'$
Output: $\mathbf{F}_{\mathrm{RF}}$

```
Calculate V, V̄, and Ū.
if M_RF ≤ r then
    for i = 1 → M_RF do
        Design f_RF^i based on ū^i using column design approach 2
    end for
else
    for w = 1 → M_RF − r do
        Design f_RF^{2w−1} and f_RF^{2w} based on ū^w using column design approach 1
    end for
    for w = M_RF − r + 1 → M_RF do
        Design f_RF^{M_RF−r+w} based on ū^w using column design approach 2
    end for
end if
```

Note that with Algorithm 2, if $M_{\mathrm{RF}} \leq r$, the M_{RF} most dominant eigen-directions are considered in the analog beamforming design, but none of them is fully spanned by $\mathbf{F}_{\mathrm{RF}}$. On the other hand, if $M_{\mathrm{RF}} > r$, all the eigen-directions are taken into account in the design, while the $(M_{\mathrm{RF}} - r)$ most dominant eigen-directions are fully spanned by $\mathbf{F}_{\mathrm{RF}}$ since each of them is spanned by two RF beamforming vectors.

Also note that if $M_{\mathrm{RF}} \geq 2r$, the above two proposed schemes both lead to the same design of the analog beamforming matrix $\mathbf{F}_{\mathrm{RF}}$, which completely spans $\bar{\mathbf{U}}$. Furthermore, since $\bar{\mathbf{U}}$ has the same column space of $\mathbf{U}$ (the left-singular space of $\mathbf{V}$), based on the proof of Proposition 4, it follows that the fully digital beamforming performance can be achieved by both proposed schemes since the sufficient conditions given in Theorem 1 are satisfied, as will be verified by the simulation results in the next section.

VII. Simulation Results

In this section, numerical results are provided to evaluate the performance of the proposed schemes for WPT with hybrid beamforming. We consider a general multi-path environment, where the fractional power ratio of the lth path is given by $\kappa_l = \frac{|\kappa_l'|}{\sum_{k=1}^{L} |\kappa_k'|}$, with $\kappa_l' \sim \mathcal{CN}(0,1)$ for $l = 1, \cdots, L$. In addition, the large-scale path-loss is set as 40 dB, i.e., $\beta = 10^{-4}$. Furthermore, the AoA and AoD of each path are assumed to be uniformly distributed in the interval $[-\pi/2,\ \pi/2]$.

We assume that the total available bandwidth for the WPT system is $B = 10$ megahertz (MHz), which is equally divided into $N = 100$ sub-bands each with bandwidth $B_{\mathrm{s}} = 100$ kilohertz (kHz). We further assume that the maximum path delay is 500 nanoseconds (ns). The number of antennas at the ET and ER are set as $M_{\mathrm{T}} = 30$ and $M_{\mathrm{R}} = 6$, respectively. The total transmit power at the ET is $P_t = 1$ Watt.

For the benchmark schemes, due to the peak power constraint at each sub-band, we first adopt the same set of selected sub-bands and their transmit power allocation as for the fully digital case. Then, for the design of analog beamformer $\mathbf{F}_{\mathrm{RF}}$, we consider two benchmark schemes. In benchmark 1, we adopt the algorithm in [36], which was proposed for wide-band wireless information transfer, instead of WPT. Specifically, each element of $\mathbf{F}_{\mathrm{RF}}$ is iteratively designed to maximize the value of $\log_2(|\mathbf{I} + \mathbf{F}_{\mathrm{RF}}^H \mathbf{H}_{\mathrm{sum}} \mathbf{F}_{\mathrm{RF}}|)$, with $\mathbf{H}_{\mathrm{sum}} = \sum_{n=1}^{N'} (\mathbf{H}_{[n]}^H \mathbf{H}_{[n]})$ obtained by simply summing up all the N' sub-bands. In benchmark 2, $\mathbf{F}_{\mathrm{RF}}$ is designed to maximize $\mathrm{tr}(\mathbf{F}_{\mathrm{RF}}^H \mathbf{H}_{\mathrm{sum}} \mathbf{F}_{\mathrm{RF}})$, which is equivalent to $\sum_{i=1}^{M_{\mathrm{RF}}} (\mathbf{f}_{\mathrm{RF}}^i)^H \mathbf{H}_{\mathrm{sum}} \mathbf{f}_{\mathrm{RF}}^i$. In this case, each column of $\mathbf{F}_{\mathrm{RF}}$ is similarly designed using the iterative algorithm given in [48]. With the obtained analog beamformer, the system is equivalent to a fully digital WPT system. Hence, the digital beamformer at each selected sub-band can be designed such that the energy symbol is transmitted via the dominant eigen-direction of the equivalent channel.

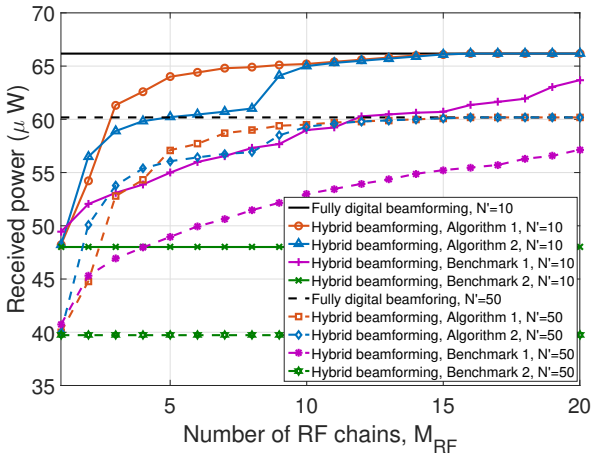

Fig. 2: The received power versus number of RF chains in sparse channel environment, with $L = 8$, and $N' = 10$ or 50.

First, Fig. 2 shows the performance of the proposed schemes versus the number of RF chains M_{RF} in a sparse channel environment, where the number of paths is set as $L = 8$. We consider two scenarios where the transmit power constraints per sub-band are set as $P_s = 100$mW and 20mW, which correspond to $N' = 10$ and $N' = 50$, respectively.

Note that according to Theorem 1, the fully digital beamforming performance in the considered setup can be achieved when the number of RF chains is no smaller than $2L = 16$. This is validated in Fig. 2 for both proposed Algorithms 1 and 2. Furthermore, it is observed that with both algorithms, the fully digital beamforming performance can be almost achieved even when the number of RF chains is slightly less than 16. This is because in sparse channel environment with few channel paths, the channel matrices over sub-bands are highly correlated, and hence the dominant eigenvectors of adjacent sub-bands are very similar. In such a case, only a few eigen-directions of the effective channel matrix over all sub-bands $\bar{\mathbf{V}}$ are dominant, and therefore a near-optimal performance can be achieved as long as those dominant eigen-directions are considered in the proposed analog beamforming designs. Furthermore, it is also observed that when the number of RF chains is small, Algorithm 2 outperforms Algorithm 1, whereas the reverse is true when the number of RF chains increases (and is

This article has been accepted for publication in a future issue of this journal, but has not been fully edited. Content may change prior to final publication. Citation information: DOI 10.1109/TWC.2018.2865313, IEEE Transactions on Wireless Communications

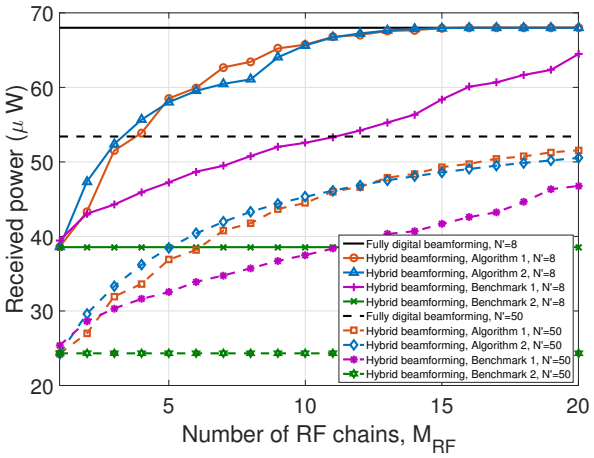

Fig. 3: The received power versus different number of RF chains in rich scattering environment, with $L = 100$ and $N' = 8$ or 50.

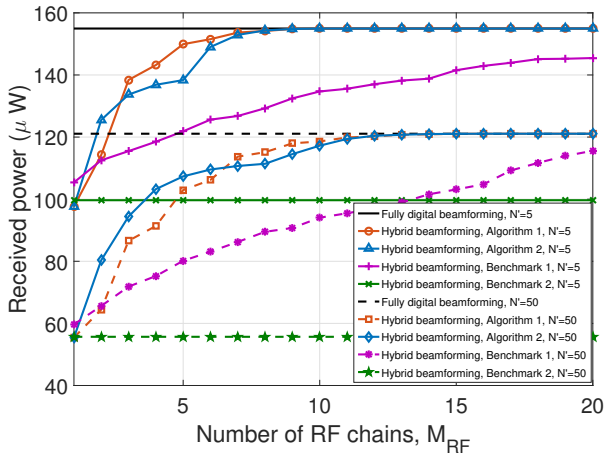

Fig. 4: The received power versus different number of RF chains for MISO system, with $L = 8$ and $N' = 5$ or 50.

less than 16). This is due to the different approaches adopted by them for the design of the analog beamforming matrix $\mathbf{F}_{\mathrm{RF}}$. Specifically, in Algorithm 1, each pair of columns in $\mathbf{F}_{\mathrm{RF}}$ are designed to fully span one dominant eigen-direction of $\bar{\mathbf{V}}$, so that $\lfloor M_{\mathrm{RF}}/2 \rfloor$ most dominant eigen-directions are fully characterized by the design. On the other hand, in Algorithm 2, each column of $\mathbf{F}_{\mathrm{RF}}$ is designed for one corresponding eigen-direction in $\bar{\mathbf{V}}$ until all eigen-directions are covered. Therefore, when the number of RF chains is small, Algorithm 2 involves more dominant eigen-directions than Algorithm 1, and hence gives better performance. However, when the number of RF chain increases, the extra RF chains in Algorithm 2 are first used for covering the non-dominant eigen-directions instead of for completely spanning the most dominant eigen-directions as in Algorithm 1, thus resulting in worse performance.

Finally, it is observed that both proposed algorithms outperform the two benchmark schemes. Moreover, for benchmark 1, while the received power also increases with the increase of the number of RF chains, it cannot achieve the same performance as the fully digital beamforming even when the condition of Theorem 1 is satisfied. This is mainly due to the fundamental difference between the rate-optimal information transfer and the energy-optimal power transfer, which also implies that the existing hybrid beamforming designs for information transfer cannot be directly used for power transfer. For benchmark 2, it is observed that the performance will not improve when the number of RF chain increases. This is because by simply maximizing the trace of $\mathbf{F}_{\mathrm{RF}}^H \mathbf{H}_{\mathrm{sum}} \mathbf{F}_{\mathrm{RF}}$, all columns of $\mathbf{F}_{\mathrm{RF}}$ would become identical, which thus does not take the advantage of multiple RF chains. In addition, note that in both benchmark schemes, the analog beamformer is designed based on the sum of the channel matrices of all selected sub-bands, and therefore the channel variations over the sub-bands are not fully exploited.

Fig. 3 shows the performance of the proposed algorithms in a rich scattering environment, where the number of channel paths L is set to be 100 and as a result the channels in different sub-bands are less correlated. We consider the peak transmit power constraints per sub-band set as $P_s = 125$ mW or $P_s = 20$ mW, which correspond to $N' = 8$ and $N' = 50$, respectively.

It is observed in Fig. 3 that when $N' = 8$, the fully digital beamforming performance can be achieved with both Algorithms 1 and 2, when the number of RF chains equals $2N' = 16$, which is consistent with Theorem 1. However, when $N' = 50$, the fully digital beamforming performance cannot be achieved even with 20 RF chains by both proposed hybrid beamforming schemes, since according to Proposition 1 and Theorem 1, the minimum number of RF chains required for achieving the optimal digital beamforming performance is $\min\{M_{\mathrm{T}}, 2N', 2L\} = 30$ in this case. Furthermore, note that in the case of $N' = 50$, Algorithm 1 gives better performance than Algorithm 2 when the number of RF chains is more than 13, which is in contrast to the sparse channel case in Fig. 2, where Algorithm 1 outperforms Algorithm 2 when the number of RF chains is no less than 5. This is because with less correlated sub-band channels, all the eigen-directions in $\bar{\mathbf{V}}$ become important and thus need to be taken into account in the hybrid beamforming design when the number of RF chains is not large.

Finally, we study the special case of MISO WPT system with $M_{\mathrm{R}} = 1$. We assume that the number of paths and the used sub-bands are $L = 8$ and $N' = 5$ or 50, respectively. It is shown in Fig. 4 that with both Algorithms 1 and 2, the fully digital beamforming performance is achieved when the number of RF chains reaches 10 and 16 for the case of $N' = 5$ and 50, respectively, which agrees with Theorem 1. Recall that according to Corollary 1, in MISO WPT system, the fully digital beamforming performance can be achieved with the number of RF chains equals $\min\{L, 2N'\}$, which implies that in this case, only $L = 8$ RF chains are needed to achieve the fully digital beamforming performance based on the hybrid beamforming design proposed in the constructive proof of Proposition 3. However, note that the proposed design for Proposition 3 is based on the specific channel parameter information such as path gains and AoDs, while the proposed algorithms only use the information of channel matrices (i.e.,

This article has been accepted for publication in a future issue of this journal, but has not been fully edited. Content may change prior to final publication. Citation information: DOI 10.1109/TWC.2018.2865313, IEEE Transactions on Wireless Communications

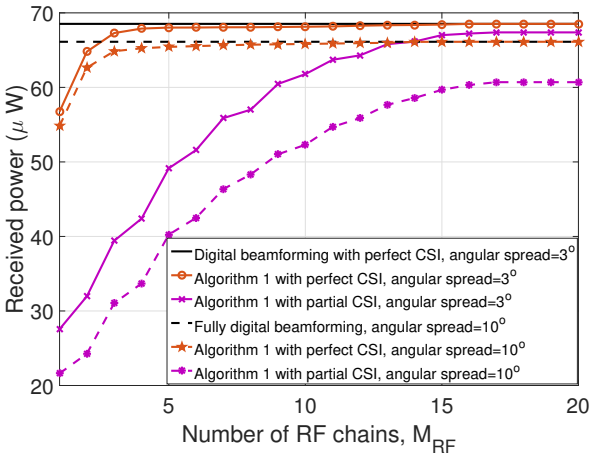

Fig. 5: The received power versus different number of RF chains based on partial CSI, with $L = 8$ and angle spread equal to 3° or 10°.

the channel frequency response) of the sub-bands without assuming the knowledge of path gains and AoDs at the ET, and therefore cannot directly satisfy the condition of Proposition 3.

Next, we consider the implementation of our proposed design in a more practical scenario, where only partial channel state information (CSI) is available at the transmitter for the design of analog beamformer. Specifically, with the cluster-based multi-path model, we assume that the AoA/AoD of each path follows the Gaussian distribution with certain mean and standard deviation, which are specified by the nominal AoA/AoD and the angular spread of the corresponding cluster, respectively [49], [50]. Furthermore, since the nominal angles are user location-based and vary much slower than the instantaneous CSI, they can be more easily estimated by the transmitter [50].

Fig. 5 shows the performance of the proposed algorithm based on only the partial CSI, where the analog beamformer is designed using Algorithm 1 based on the nominal AoAs/AoDs. In the simulation, we assume that the nominal angles of each path are randomly generated from the interval $[-\pi/2,\ \pi/2]$, and the angular spreads of all clusters are the same.

It is observed in Fig. 5 that the performance of Algorithm 1 based on partial CSI improves as the number of RF chains increases, and the performance gap compared to that with perfect CSI is closely related to the number of RF chains and the angular spread. Specifically, the proposed algorithm can still provide good performance with only partial CSI when the number of RF chains is sufficiently large and the angular spread is small. This is expected since small number of RF chains gives few design degrees of freedom in the digital domain and large angular spread causes large deviations of the actual angles from nominal angles.

VIII. Conclusion

In this paper, we studied a novel WPT system based on hybrid analog/digital beamforming that is applicable with limited number of RF chains at the ET. We first derived the sufficient number of RF chains that are required at the ET to achieve the fully digital beamforming performance, in terms of the number of sub-bands used and the number of channel paths. Moreover, for the cases with insufficient RF chains, two efficient algorithms were proposed for the analog beamforming design. Simulation results show that the two proposed algorithms outperform one another in different regimes of number of RF chains, and both algorithms converge to the fully digital beamforming performance when the number of RF chains becomes sufficiently large. In this paper, the point-to-point WPT system was considered. It would be interesting to extend the analysis and design in this paper to the more general multi-user systems. Another promising research direction is to study the hybrid design under the more practical non-linear RF energy harvesting model. Furthermore, the practical scenarios with only partial or limited CSI at the ET also require more in-depth investigations.

Appendix A

To prove Lemma 1, we first make the change of variables by letting

$$\mathbf{F}_{\mathrm{BB},n} = (\mathbf{F}_{\mathrm{RF}}^H\mathbf{F}_{\mathrm{RF}})^{-\frac{1}{2}}\bar{\mathbf{F}}_{\mathrm{BB},n},\ n = 1, \cdots, N, \tag{20}$$

and problem (P2) becomes

$$\begin{aligned} \underset{\mathbf{F}_{\mathrm{RF}},\{\bar{\mathbf{F}}_{\mathrm{BB},n},p_n\}}{\mathrm{Max.}} \quad & \sum_{n=1}^{N}\frac{p_n}{K_n}\mathrm{tr}(\bar{\mathbf{F}}_{\mathrm{BB},n}^H\mathbf{H}_{eq,n}^H\mathbf{H}_{eq,n}\bar{\mathbf{F}}_{\mathrm{BB},n}) \\ \text{s. t.} \quad & (11), \\ & \mathrm{tr}(\bar{\mathbf{F}}_{\mathrm{BB},n}\bar{\mathbf{F}}_{\mathrm{BB},n}^H) = K_n, \forall n, \\ & \sum_{n=1}^{N} p_n \le P_t, \quad 0 \le p_n \le P_s, \forall n. \end{aligned} \tag{21}$$

where $\mathbf{H}_{eq,n} = \mathbf{H}_n\mathbf{F}_{\mathrm{RF}}(\mathbf{F}_{\mathrm{RF}}^H\mathbf{F}_{\mathrm{RF}})^{-\frac{1}{2}}$ denotes the equivalent channel matrix at sub-band n.

Using the same approach as [35], it can be shown that the problem (21) is equivalent to problem (P2) . Furthermore, note that for any given $\mathbf{F}_{\mathrm{RF}}$, problem (21) is similar to problem (P1) with fully digital structure, and hence the optimal solution of $\mathbf{F}_{\mathrm{BB},n}$ can be written as

$$\bar{\mathbf{F}}_{\mathrm{BB},n} = \hat{\mathbf{v}}_n^*, n = 1, \cdots, N, \tag{22}$$

where $\hat{\mathbf{v}}_n^*$ denotes the eigenvector corresponding to the dominant eigenvalue of $\mathbf{H}_{eq,n}^H\mathbf{H}_{eq,n}$.

Finally, by substituting (22) into (20), the expression (15) in Lemma 1 is obtained.

Appendix B

To show Proposition 2, note that for LoS channel with $L = 1$ and $\tau_1 = 0$, the MIMO channel at sub-band n in (3) reduces to

$$\mathbf{H}_n = \alpha_{1n}\mathbf{a}(\varphi_1^r, \theta_1^r)\mathbf{b}^H(\varphi_1^t, \theta_1^t),\ n = 1, \cdots, N. \tag{23}$$

Therefore, for LoS channels, the MIMO channel matrices in all sub-bands are identical, i.e., we have frequency-flat channel in LoS environment, as expected. Therefore, the dominant

This article has been accepted for publication in a future issue of this journal, but has not been fully edited. Content may change prior to final publication. Citation information: DOI 10.1109/TWC.2018.2865313, IEEE Transactions on Wireless Communications

eigenvectors of the MIMO channels for all sub-bands are identical, which are given by

$$\mathbf{v}_n^* = \mathbf{v}_{\max}(\mathbf{H}_n^H \mathbf{H}_n) = \mathbf{b}(\varphi_1^t, \theta_1^t), \forall n = 1, \cdots, N. \quad (24)$$

Hence, (17) can be satisfied with a single RF chain by letting

$$\mathbf{f}_{\mathrm{RF}} = \mathbf{b}(\varphi_1^t, \theta_1^t) = \mathbf{v}_n^*, \forall n = 1, \cdots, N, \quad (25)$$

where $\mathbf{f}_{\mathrm{RF}} \in \mathbb{C}^{M_{\mathrm{T}} \times 1}$ represents the analog beamforming vector. Note that $\mathbf{f}_{\mathrm{RF}}$ in (25) satisfies the constant-modulus constraint since all elements in $\mathbf{b}(\varphi_1^t, \theta_1^t)$ have the magnitudes equal to $1/M_{\mathrm{T}}$. The proof of Proposition 2 is thus completed.

APPENDIX C

To prove Proposition 3, it is sufficient to show that (17) can be satisfied if $M_{\mathrm{RF}} = L$, since for $M_{\mathrm{RF}} > L$, the same design can be applied by simply discarding the extra RF chains.

Note that with MISO system with $M_{\mathrm{R}} = 1$, the channel $\mathbf{H}_n$ in (3) reduces to a row vector, which is thus denoted as $\mathbf{h}_n^H \in \mathbb{C}^{1 \times M_{\mathrm{T}}}$. Furthermore, we have

$$\mathbf{h}_n^H = \boldsymbol{\alpha}_n^H \mathbf{B}^H, \quad (26)$$

where $\boldsymbol{\alpha}_n^H = [\alpha_{1n}, \cdots, \alpha_{Ln}]$, and $\mathbf{B} = \left[\mathbf{b}(\varphi_1^t, \theta_1^t) \ \cdots \ \mathbf{b}(\varphi_L^t, \theta_L^t) \right]$, with $\mathbf{b}(\varphi_l^t, \theta_l^t)$ defined in (2).

As a result, the dominant eigenvectors of the channel at each sub-band can be expressed as

$$\mathbf{v}_n^* = \frac{\mathbf{h}_n}{\|\mathbf{h}_n\|} = \frac{1}{\|\mathbf{h}_n\|} \mathbf{B} \boldsymbol{\alpha}_n, n = 1, \cdots, N, \quad (27)$$

and hence the condition in (17) can be expressed as

$$\mathbf{F}_{\mathrm{RF}} \mathbf{f}_{\mathrm{BB},[n]} = \mathbf{v}_{[n]}^* = \mathbf{B} \frac{1}{\|\mathbf{h}_{[n]}\|} \boldsymbol{\alpha}_n, n = 1, \cdots, N'. \quad (28)$$

Since the elements in $\mathbf{B} \in \mathbb{C}^{M_{\mathrm{T}} \times L}$ have constant modulus, (28) can be satisfied by letting $\mathbf{F}_{\mathrm{RF}} = \mathbf{B}$ and $\mathbf{f}_{\mathrm{BB},[n]} = \frac{1}{\|\mathbf{h}_{[n]}\|} \boldsymbol{\alpha}_n$, $n = 1, \cdots, N'$. The proof of Proposition 3 is thus completed.

APPENDIX D

To prove Proposition 4, let $r = \mathrm{rank}(\mathbf{V})$, it is sufficient to show that when $M_{\mathrm{RF}} = 2r$, there exists $\mathbf{F}_{\mathrm{RF}} \in \mathbb{C}^{M_{\mathrm{T}} \times 2r}$ and $\mathbf{f}_{\mathrm{BB},[n]} \in \mathbb{C}^{2r \times 1}$, $n = 1, \cdots, N'$, which satisfy (17). This is because if $M_{\mathrm{RF}} > 2r$, the same design can be applied by simply discarding those redundant RF chains.

Denote by $\mathbf{V} = \mathbf{U} \boldsymbol{\Gamma} \mathbf{W}^H$ the (reduced) singular value decomposition (SVD) of $\mathbf{V}$, where $\mathbf{U} \in \mathbb{C}^{M_{\mathrm{T}} \times r}$ and $\mathbf{W} \in \mathbb{C}^{N' \times r}$, each of which consists of orthonomal columns spanning the left and right singular space of $\mathbf{V}$, respectively, and $\boldsymbol{\Gamma} = \mathrm{diag}(\gamma_1, \cdots, \gamma_r)$, with $\gamma_1 \geq \cdots \geq \gamma_r$. Therefore, the matrix $\mathbf{U}$ has rank of r and constitutes a basis of $\mathbf{V}$. In the following, we first design $\mathbf{F}_{\mathrm{RF}}$ such that a matrix $\mathbf{F} \in \mathbb{C}^{2r \times r}$ can be found to satisfy

$$\mathbf{F}_{\mathrm{RF}} \mathbf{F} = \mathbf{U}. \quad (29)$$

Note that (29) implies that the column space of $\mathbf{U}$ is spanned by $\mathbf{F}_{\mathrm{RF}}$ as each column of $\mathbf{U}$ can be written as a linear combination of the columns in $\mathbf{F}_{\mathrm{RF}}$.

To this end, denote by $\mathbf{f}^n$ the nth column of $\mathbf{F}$, we first set $\mathbf{f}^n$ as a $2r \times 1$ vector with non-zero variables at the $(2n-1)$th and $(2n)$th elements, i.e.,

$$\mathbf{f}^n = \left[\ \mathbf{0}^T \quad f_{2n-1} \quad f_{2n} \quad \mathbf{0}^T \ \right]^T, \ n = 1, \cdots, r. \quad (30)$$

Hence, (29) can be expressed as

$$f_{2n-1} \mathbf{f}_{\mathrm{RF}}^{2n-1} + f_{2n-1} \mathbf{f}_{\mathrm{RF}}^{2n} = \mathbf{u}^n, n = 1, \cdots, r, \quad (31)$$

where $\mathbf{u}^n$ and $\mathbf{f}_{\mathrm{RF}}^n$ denote the nth columns of $\mathbf{U}$ and $\mathbf{F}_{\mathrm{RF}}$, respectively. Note that (31) indicates that the $(2n-1)$th and $(2n)$th columns of $\mathbf{F}_{\mathrm{RF}}$ are designed only based on the nth column of $\mathbf{U}$.

Let the ith element of $\mathbf{f}_{\mathrm{RF}}^{2n-1}$ and $\mathbf{f}_{\mathrm{RF}}^{2n}$ be expressed as $f_{\mathrm{RF},i}^{2n-1} = \frac{1}{\sqrt{M_{\mathrm{T}}}} e^{j\sigma_{2n-1,i}}$ and $f_{\mathrm{RF},i}^{2n} = \frac{1}{\sqrt{M_{\mathrm{T}}}} e^{j\sigma_{2n,i}}$, respectively, $i = 1, \cdots, M_{\mathrm{T}}$. Furthermore, let the ith element of $\mathbf{u}^n$ be expressed as $u_i^n = \mu_{n,i} e^{j\omega_{n,i}}$, where $\mu_{n,i}$ is a real number denoting the modulus of u_i^n. Then, (31) can be written as

$$f_{2n-1} \frac{1}{\sqrt{M_{\mathrm{T}}}} e^{j\sigma_{2n-1,i}} + f_{2n} \frac{1}{\sqrt{M_{\mathrm{T}}}} e^{j\sigma_{2n,i}} = \mu_{n,i} e^{j\omega_{n,i}}, \quad (32)$$

where $i = 1, \cdots, M_{\mathrm{T}}$ and $n = 1, \cdots, r$.

According to [32], (32) can be satisfied by letting $f_{2n-1} = f_{2n} = \sqrt{M_{\mathrm{T}}} \mu_{n,i}^{\max}$, where $\mu_{n,i}^{\max} = \max_i \{\mu_{n,i}\}$, $\sigma_{2n-1,i} = \omega_{n,i} - \cos^{-1}(\frac{\mu_{n,i}}{2\mu_{n,i}^{\max}})$, and $\sigma_{2n,i} = \omega_{n,i} + \cos^{-1}(\frac{\mu_{n,i}}{2\mu_{n,i}^{\max}})$, $\forall n = 1 \cdots, r$.

Next, we design $\mathbf{F}_{\mathrm{BB}} = \left[\ \mathbf{f}_{\mathrm{BB},[1]} \ \cdots \ \mathbf{f}_{\mathrm{BB},[N']} \ \right]$ such that the condition in (17) is satisfied. Note that by concatenating all equations for the N' sub-bands, (17) can be compactly written as

$$\mathbf{F}_{\mathrm{RF}} \mathbf{F}_{\mathrm{BB}} = \mathbf{V}. \quad (33)$$

With $\mathbf{F}_{\mathrm{RF}}$ designed to satisfy (29) and $\mathbf{V} = \mathbf{U} \boldsymbol{\Gamma} \mathbf{W}^H$, (33) can be satisfied by letting $\mathbf{F}_{\mathrm{BB}} = \mathbf{F} \boldsymbol{\Gamma} \mathbf{W}^H$. The proof of Proposition 4 is thus completed.

APPENDIX E

To prove Lemma 2, it is sufficient to show that $\mathrm{rank}(\mathbf{V}) \leq L$, since $\mathrm{rank}(\mathbf{V}) \leq N'$ is obvious as $\mathbf{V}$ has only N' columns. Let $\boldsymbol{\Lambda} = \mathrm{diag}(\lambda_{\max,[1]}, \cdots, \lambda_{\max,[N']})$. Note that the rank of $\mathbf{V} \triangleq \left[\ \mathbf{v}_{[1]}^* \ \cdots \ \mathbf{v}_{[N']}^* \ \right]$ is the same as that of $\mathbf{V}\boldsymbol{\Lambda}$, as $\boldsymbol{\Lambda}$ is an $N' \times N'$ full-rank matrix.

Hence, in the following we study the rank of $\mathbf{V}\boldsymbol{\Lambda}$. In particular, based on the definition of eigenvectors, we have

$$\begin{aligned} \mathbf{V}\boldsymbol{\Lambda} &= \left[\ \lambda_{\max,[1]} \mathbf{v}_{[1]}^* \ \cdots \ \lambda_{\max,[N']} \mathbf{v}_{[N']}^* \ \right] \\ &= \left[\ \mathbf{H}_{[1]}^H \mathbf{H}_{[1]} \mathbf{v}_{[1]}^* \ \cdots \ \mathbf{H}_{[N']}^H \mathbf{H}_{[N']} \mathbf{v}_{[N']}^* \ \right], \end{aligned} \quad (34)$$

where $\mathbf{H}_{[n]}$ is defined in (3), which can be further expressed as

$$\mathbf{H}_{[n]} = \mathbf{A} \mathrm{diag}(\boldsymbol{\alpha}_{[n]}^H) \mathbf{B}^H, \quad (35)$$

with $\mathbf{A} = \left[\ \mathbf{a}(\varphi_1^r, \theta_1^r) \ \cdots \ \mathbf{a}(\varphi_L^r, \theta_L^r) \ \right]$, $\boldsymbol{\alpha}_n^H = [\alpha_{1n}, \ \cdots, \ \alpha_{Ln}]$,
and $\mathbf{B} = \left[\ \mathbf{b}(\varphi_1^t, \theta_1^t) \ \cdots \ \mathbf{b}(\varphi_L^t, \theta_L^t) \ \right]$.

By substituting (35) into (34), we have

$$\mathbf{V}\boldsymbol{\Lambda} = \mathbf{B}\mathbf{D}, \quad (36)$$

where

$$\mathbf{D} = \Big[\mathrm{diag}(\boldsymbol{\alpha}_{[1]}^H)^H \mathbf{A}^H \mathbf{A} \mathrm{diag}(\boldsymbol{\alpha}_{[1]}^H) \mathbf{B}^H \mathbf{v}_{[1]}^* \ \cdots \ \mathrm{diag}(\boldsymbol{\alpha}_{[N']}^H)^H \mathbf{A}^H \mathbf{A} \mathrm{diag}(\boldsymbol{\alpha}_{[N']}^H) \mathbf{B}^H \mathbf{v}_{[N']}^* \Big].$$

Since $\mathbf{B} \in \mathbb{C}^{M_{\mathrm{T}} \times L}$, we have $\mathrm{rank}(\mathbf{B}) \leq L$. Therefore, $\mathrm{rank}(\mathbf{V}) = \mathrm{rank}(\mathbf{V}\boldsymbol{\Lambda}) = \mathrm{rank}(\mathbf{BD}) \leq \mathrm{rank}(\mathbf{B}) \leq L$. The proof of Lemma 2 is thus completed.

REFERENCES

[1] S. Bi, C. K. Ho, and R. Zhang, "Wireless powered communication: opportunities and challenges," *IEEE Commun. Magazine*, vol. 53, no. 4, pp.117-125, Apr. 2015.

[2] Y. Zeng, B. Clerckx, and R. Zhang, "Communications and signals design for wireless power transmission," *IEEE Trans. Commun.*, vol. 65, no. 5, pp. 2264-2290, May, 2017.

[3] G. A. Covic and J. T. Boys, "Inductive power transfer," *Proc. IEEE*, vol. 101, no. 6, pp. 1276-1289, Jun. 2013.

[4] S. Y. Hui, "Planar wireless charging technology for portable electronic products and Qi," *Proc. IEEE*, vol. 101, no. 6, pp. 1290-1301, Jun. 2013.

[5] A. Kurs, A. Karalis, R. Moffatt, J. D. Joannopoulos, P. Fisher, and M. Soljacic, "Wireless power transfer via strongly coupled magnetic resonances," *Science*, vol. 317, no. 5834, pp. 83-86, Jul. 2007.

[6] G. Yang, M. R. V. Moghadam, and R. Zhang, "Magnetic MIMO signal processing and optimization for wireless power transfer," *IEEE Trans. Sig. Process.*, vol. 65, no. 11, pp. 2860-2874, Jun. 2017.

[7] R. Zhang and C. K. Ho, "MIMO broadcasting for simultaneous wireless information and power transfer," *IEEE Trans. Wireless Commun.*, vol. 12, no. 5, pp. 1989-2001, May 2013.

[8] N. Shinohara, "Beam control technologies with a high-efficiency phased array for microwave power transmission in Japan," *Proc. IEEE*, vol. 101, no. 6, pp. 1448-1463, Jun. 2013.

[9] J. Xu and R. Zhang, "Energy beamforming with one-bit feedback," *IEEE Trans. Signal Process.*, vol. 62, no. 20, pp. 5370-5381, Oct. 2014.

[10] Y. Zeng and R. Zhang, "Optimized training design for wireless energy transfer," *IEEE Trans. Commun.*, vol. 63, no. 2, pp. 536-550, Feb. 2015.

[11] G. Yang, C. K. Ho, R. Zhang and Y. L. Guan, "Throughput optimization for massive MIMO systems powered by wireless energy transfer," *IEEE J. Sel. Areas Commun.*, vol. 33, no. 8, pp. 1640-1650, Aug. 2015.

[12] S. Bi, Y. Zeng, and R. Zhang, "Wireless powered communication networks: an overview," *IEEE Trans. Wireless Commun.*, vol. 23, no. 2, pp. 10-18, Apr. 2016.

[13] S. Kashyap, E. Bjornson, and E. G. Larsson, "On the feasibility of wireless energy transfer using massive antenna arrays," *IEEE Trans. Wireless Commun.*, vol. 15, no. 5, pp. 3466-3480, May 2016.

[14] L. Yang, Y. Zeng, and R. Zhang, "In-band wireless information and power transfer with lens antenna array," *IEEE Commun. Lett.*, vol. 21, no. 1, pp. 100-103, Jan. 2017.

[15] P. Yedavalli, T. Riihonen, X. D. Wang, and J. M. Rabaey, "Far-field RF wireless power transfer with blind adaptive beamforming for internet of things devices," *IEEE Access*, vol. 5, pp. 1743-1752, Mar. 2017.

[16] K. Choi, D. Kim, and M. Chung, "Received power-based channel estimation for energy beamforming in multiple-antenna RF energy transfer system," *IEEE Trans. Sig. Process.*, vol. 65, no. 6, pp. 1461-1476, Mar. 2017.

[17] S. Lee, Y. Zeng, and R. Zhang, "Retrodirective multi-user wireless power transfer with massive MIMO," *IEEE Wireless Commun. Lett.*, vol. 7, no. 1, pp. 54-57, Feb. 2018.

[18] J. Zhang, T. Wei, X. Yuan, and R. Zhang, "Multi-antenna constant envelope wireless power transfer," *IEEE Trans. Green Commun. and Networking*, vol. 1, no. 4, pp. 458-467, Dec. 2017.

[19] X. Zhou, R. Zhang, and C. K. Ho, "Wireless information and power transfer in multiuser OFDM systems," *IEEE Trans. Wireless Commun.*, vol. 13, no. 4, pp. 2282-2294, Apr. 2014.

[20] Y. Zeng and R. Zhang, "Optimized training for net energy maximization in multi-antenna wireless energy transfer over frequency-selective channel," *IEEE Trans. Commun.*, vol. 63, no. 6, pp. 2360-2373, Jun. 2015.

[21] M. Ku, Y. Han, H. Lai, Y. Chen, and K. J. Ray Liu, "Power waveforming: wireless power transfer beyond time reversal," *IEEE Trans. Sig. Process.*, vol. 64, no. 22, pp. 5819-5834, Nov. 2016.

[22] S. Bi and R. Zhang, "Distributed charging control in broadband wireless power transfer networks," *IEEE J. Sel. Areas Commun.*, vol. 34, no. 12, pp. 3380-3393, Dec. 2016.

[23] S. Hur, T. Kim, D. Love, J. Krogmeier, T. Thomas, and A. Ghosh, "Millimeter wave beamforming for wireless backhaul and access in small cell network," *IEEE Trans. Commun.*, vol. 61, no. 10, pp. 4391-4403, Oct. 2013.

[24] Y. Zeng and R. Zhang, "Millimeter wave MIMO with lens antenna array: a new path division multiplexing paradigm," *IEEE Trans. Commun.*, vol. 64, no. 4, pp. 1557-1571, Apr. 2016.

[25] L. Yang, Y. Zeng, and R. Zhang, "Efficient channel estimation for millimeter wave MIMO with limited RF chains," *in Proc. IEEE Inter. Conf. on Commun.* (ICC 2016), Kuala Lumpur, Malaysia, 23–27 May 2016.

[26] Y. Zeng and R. Zhang, "Cost-effective millimeter wave communications with lens antenna array", *IEEE Wireless Commun. Mag.*, vol. 24, no. 4, pp. 81-87, Aug., 2017.

[27] L. Yang, Y. Zeng and R. Zhang, "Channel estimation for millimeter wave MIMO communications with lens antenna arrays," *IEEE Trans. Vehicular Technology*, vol. 67, no. 4, pp. 3239-3251, Apr., 2018.

[28] Y. Zeng, L. Yang, and R. Zhang, "Multi-user millimeter wave MIMO with full dimensional lens antenna array," *IEEE Trans. Wireless Commun.*, vol. 7, no. 4, pp. 2800-2814, Apr., 2018.

[29] X. Zhang, F. Molisch, and S. Kung, "Variable-phase-shift-based RF-baseband codesign for MIMO antenna selection," *IEEE Trans. Sig. Process.*, vol. 53, no. 11, pp. 4091-4103, Nov. 2005.

[30] V. Venkateswaran and A. J. van der Veen, "Analog beamforming in MIMO communications with phase shift networks and online channel estimation," *IEEE Trans. Signal Process.*, vol. 58, no. 8, pp. 4131-4143, Aug. 2010.

[31] O. Ayach, S. Rajagopal, S. Abu-Surra, Z. Pi, and R. Heath Jr., "Spatially sparse precoding in millimeter wave MIMO systems," *IEEE Trans. Wireless Commun.*, vol. 13, no. 3, pp. 1499-1513, Mar. 2014.

[32] F. Sohrabi and W. Yu, "Hybrid digital and analog beamforming design for large-scale antenna arrays," *IEEE J. Sele. Topics. Sig. Process.*, vol. 10, no. 3, pp. 503-513, Apr. 2016.

[33] A. M. Sayeed and V. Raghavan, "Maximizing MIMO capacity in sparse multipath with reconfigurable antenna arrays," *IEEE J. Sele. Topics Sig. Process.*, vol. 1, no. 1, pp. 156-166, Jun. 2007.

[34] A. Alkhateeb, G. Leus, and R. Heath Jr., "Limited feedback hybrid precoding for multi-user millimeter wave system," *IEEE Trans. Wireless Commun.*, vol. 14, no. 11, pp. 6481-6494, Nov. 2015.

[35] A. Alkhateeb and R. Heath, Jr., "Frequency selective hybrid precoding for limited feedback millimeter wave systems," *IEEE Trans. Commun.*, vol. 64, no. 5, pp. 1801-1818, May 2016.

[36] F. Sohrabi and W. Yu, "Hybrid analog and digital beamforming for mmWave OFDM large-scale antenna arrays," *IEEE J. Sele. Areas Commun.*, vol. 35, no. 7, pp. 1432-1443, Jul. 2017.

[37] O. T. Demir and T. E. Tuncer, "Antenna selection and hybrid beamforming for simultaneous wireless information and power transfer in multi-group multicasting systems," *IEEE Trans. Wireless Commun.*, vol. 15, no. 10, pp. 6948-6962, Oct. 2016.

[38] A. Li and C. Masouros, "Energy efficient SWIPT: from fully-digital to hybrid analog-digital beamforming," *IEEE Trans. Vehicular Technology*, vol. 67, no. 4, pp. 3390-3405, Apr., 2018.

[39] C. Balanis, Antenna Theory, Wiley, 1997.

[40] K. Venugopal, N. Gonzalez-Prelcic, and R. W. Heath, Jr., "Optimality of frequency flat precoding in frequency selective millimeter wave channels," *IEEE Wireless Commun. Lett.*, vol. 6, no. 3, pp. 330-333, May 2017.

[41] B. Yang, K. B. Letaief, R. S. Cheng, and Z. Cao, "Channel estimation for OFDM transmission in multipath fading channels based on parametric channel modeling," *IEEE Trans. Commun.*, vol. 49, no. 3, pp. 467-478, Mar. 2001.

[42] Recommendations, I. T. U. R., "Propagation data and prediction methods for the planning of indoor radiocommunication systems and radio local area networks in the frequency range 900MHz to 100GHz," ITU Recommendations, 2001.

[43] B. Clerckx and E. Bayguzina, "Waveform design for wireless power transfer," *IEEE Trans. Signal Process.*, vol. 64, no. 23, pp. 6313-6328, Dec. 2016.

[44] M. R. V. Moghadam, Y. Zeng, and R. Zhang, "Waveform optimization for radio-frequency wireless power transfer," *IEEE International Workshop on Signal Processing Advances for Wireless Communications*, Hokkaido, Japan, 3–6 Jul. 2017.

[45] FCC Rules and Regulations Part 15 Section 247, Operation within the bands 902-928 MHz, 2400-2483.5 MHz, and 5725-5850 MHz.

[46] M. Akdeniz, Y. Liu, M. Samimi, S. Sun, S. Rangan, T. Rappaport, and E. Erkip, "Millimeter wave channel modeling and cellular capacity evaluation," *IEEE J. Sel. Areas Commun.*, vol. 32, no. 6, pp. 1194-1206, Jun. 2014.

[47] J. Liang, P. Stoica, Y. Jing, and J. Li, "Phase retrieval via the alternating direction method of multipliers," *IEEE Signal Process. Lett.*, vol. 25, no. 1, pp. 5-9, Jan. 2018.
[48] Z. Pi, "Optimal transmitter beamforming with per-antenna power constraints," *Proc. IEEE Int. Conf. Commun.* (ICC 2012), Ottawa, ON, Canada, 2012, pp. 3779-3784.
[49] M. Souden, S. Affes, and J. Benesty, "A two-stage approach to estimate the angle of arrival and the angular spreads of locally scattered sources," *IEEE Trans. Signal Process.*, vol. 56, no. 5, pp. 1968-1983, May 2018.
[50] H. Yin, D. Gesbert, M. Filippou, and Y. Liu, "A coordinated approach to channel estimation in large-scale multiple-antenna systems," *IEEE J. Sel. Areas Commun.*, vol. 31, no. 2, pp. 264-273, Feb. 2013.

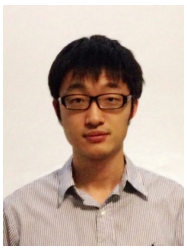

Lu Yang (S'12-M'15) received his B.S. degree in information science and engineering from Southeast University, Nanjing, China, in 2007. He received his M.S. degree and PhD degree in 2010 and 2015, respectively, both from the School of Electrical Engineering and Telecommunications, The University of New South Wales, Sydney, Australia. He was a Research Fellow at the Department Electrical and Computer Engineering, Naitional Univeristy of Singapore, in 2015-2017. He is currently with The University of New South Wales as a Research Associate. He was a visiting student at the University of California, Irvine and The Chinese University of Hong Kong in 2012 and 2013, respectively. He received 2015 IEEE Wireless Communications Letters Exemplary Reviewer Award, and the Best Paper Award for the 3rd IEEE International Conference on Wireless Communications and Signal Processing. His research interests include interference alignment, wireless power transfer, millimeter wave communications, and drone communications.

Yong Zeng (S'12-M'14) is a Lecturer at the School of Electrical and Information Engineering, The University of Sydney. He received the Bachelor of Engineering (First-Class Honours) and Ph.D. degrees from the Nanyang Technological University, Singapore, in 2009 and 2014, respectively. From 2013 to 2018, he worked as a Research Fellow and Senior Research Fellow at the Department of Electrical and Computer Engineering, National University of Singapore. His research interest includes UAV communications, wireless power transfer, massive MIMO and millimeter wave communications, and multi-user MIMO interfering communications. He has published over 70 IEEE top-tier journal and conference papers, which have attracted more than 2000 Google Scholar citations. He is the recipient of the 2017 IEEE Communications Society Heinrich Hertz Prize Paper Award, 2017 IEEE Transactions on Wireless Communications Best Reviewer, 2015 and 2017 IEEE Wireless Communications Letters Exemplary Reviewer, and the Best Paper Award for the 10th International Conference on Information, Communications and Signal Processing. He serves as an Associate Editor of IEEE Access, Leading Guest Editor of IEEE Wireless Communications on "Integrating UAVs into 5G and Beyond" and China Communications on "Network-Connected UAV Communications". He is the workshop co-chair for two workshops in ICC 2018 and the 23rd Asia-Pacific Conference on Communications (APCC).

Rui Zhang (S'00-M'07-SM'15-F'17) received the B.Eng. (first-class Hons.) and M.Eng. degrees from the National University of Singapore, Singapore, and the Ph.D. degree from the Stanford University, Stanford, CA, USA, all in electrical engineering.

From 2007 to 2010, he worked as a Research Scientist with the Institute for Infocomm Research, ASTAR, Singapore. Since 2010, he has joined the Department of Electrical and Computer Engineering, National University of Singapore, where he is now a Dean's Chair Associate Professor in the Faculty of Engineering. He has authored over 300 papers. He has been listed as a Highly Cited Researcher (also known as the World's Most Influential Scientific Minds), by Thomson Reuters since 2015. His research interests include wireless information and power transfer, drone communication, wireless eavesdropping and spoofing, energy-efficient and energy-harvesting-enabled wireless communication, multiuser MIMO, cognitive radio, and optimization methods.

He was the recipient of the 6th IEEE Communications Society Asia-Pacific Region Best Young Researcher Award in 2011, and the Young Researcher Award of National University of Singapore in 2015. He was the co-recipient of the IEEE Marconi Prize Paper Award in Wireless Communications in 2015, the IEEE Communications Society Asia-Pacific Region Best Paper Award in 2016, the IEEE Signal Processing Society Best Paper Award in 2016, the IEEE Communications Society Heinrich Hertz Prize Paper Award in 2017, the IEEE Signal Processing Society Donald G. Fink Overview Paper Award in 2017, and the IEEE Technical Committee on Green Communications Computing (TCGCC) Best Journal Paper Award in 2017. His coauthored paper received the IEEE Signal Processing Society Young Author Best Paper Award in 2017. He served for over 30 international conferences as TPC Co-Chair or Organizing Committee Member, and as the guest editor for 3 special issues in IEEE Journal of Selected Topics in Signal Processing and IEEE Journal on Selected Areas in Communications. He was an elected member of the IEEE Signal Processing Society SPCOM (2012-2017) and SAM (2013-2015) Technical Committees, and served as the Vice Chair of the IEEE Communications Society Asia-Pacific Board Technical Affairs Committee (2014-2015). He served as an Editor for the IEEE TRANSACTIONS ON WIRELESS COMMUNICATIONS (2012-2016), the IEEE JOURNAL ON SELECTED AREAS IN COMMUNICATIONS: Green Communications and Networking Series (2015-2016), and the IEEE TRANSACTIONS ON SIGNAL PROCESSING (2013-2017). He is now an Editor for the IEEE TRANSACTIONS ON COMMUNICATIONS and the IEEE TRANSACTIONS ON GREEN COMMUNICATIONS AND NETWORKING. He serves as a member of the Steering Committee of the IEEE Wireless Communications Letters.